Journal of
Fungi

Fungal Melanin and the Mammalian Immune System

Volume 7 · Issue 4 | April 2021

MDPI
mdpi.com/journal/jof
ISSN 2227-9032

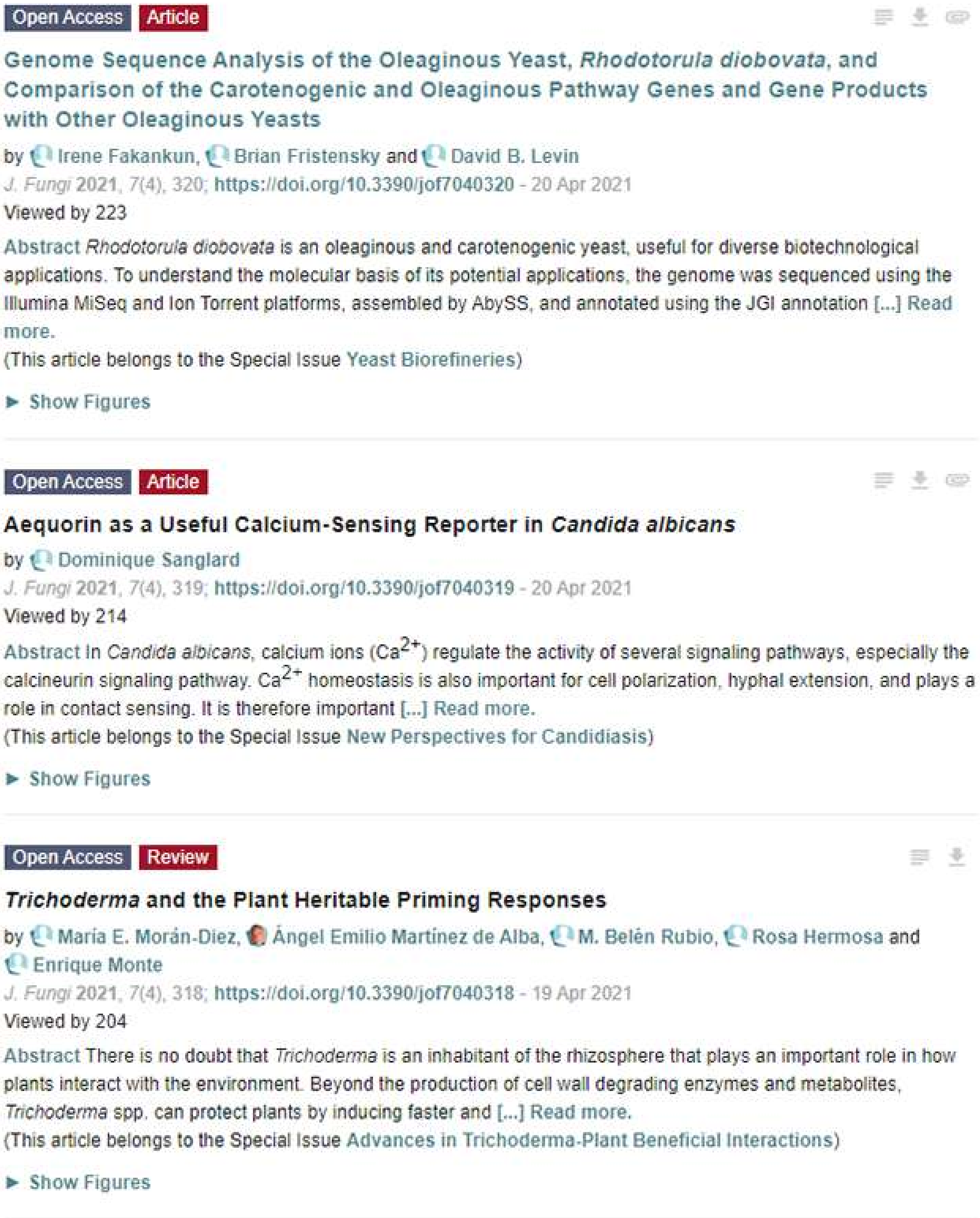

Open Access Article

Genome Sequence Analysis of the Oleaginous Yeast, *Rhodotorula diobovata*, and Comparison of the Carotenogenic and Oleaginous Pathway Genes and Gene Products with Other Oleaginous Yeasts

by Irene Fakankun, Brian Fristensky and David B. Levin

J. Fungi **2021**, *7*(4), 320; https://doi.org/10.3390/jof7040320 - 20 Apr 2021

Viewed by 223

Abstract *Rhodotorula diobovata* is an oleaginous and carotenogenic yeast, useful for diverse biotechnological applications. To understand the molecular basis of its potential applications, the genome was sequenced using the Illumina MiSeq and Ion Torrent platforms, assembled by AbySS, and annotated using the JGI annotation [...] Read more.

(This article belongs to the Special Issue Yeast Biorefineries)

► Show Figures

Open Access Article

Aequorin as a Useful Calcium-Sensing Reporter in *Candida albicans*

by Dominique Sanglard

J. Fungi **2021**, *7*(4), 319; https://doi.org/10.3390/jof7040319 - 20 Apr 2021

Viewed by 214

Abstract In *Candida albicans*, calcium ions (Ca^{2+}) regulate the activity of several signaling pathways, especially the calcineurin signaling pathway. Ca^{2+} homeostasis is also important for cell polarization, hyphal extension, and plays a role in contact sensing. It is therefore important [...] Read more.

(This article belongs to the Special Issue New Perspectives for Candidiasis)

► Show Figures

Open Access Review

Trichoderma and the Plant Heritable Priming Responses

by María E. Morán-Diez, Ángel Emilio Martínez de Alba, M. Belén Rubio, Rosa Hermosa and Enrique Monte

J. Fungi **2021**, *7*(4), 318; https://doi.org/10.3390/jof7040318 - 19 Apr 2021

Viewed by 204

Abstract There is no doubt that *Trichoderma* is an inhabitant of the rhizosphere that plays an important role in how plants interact with the environment. Beyond the production of cell wall degrading enzymes and metabolites, *Trichoderma* spp. can protect plants by inducing faster and [...] Read more.

(This article belongs to the Special Issue Advances in Trichoderma-Plant Beneficial Interactions)

► Show Figures

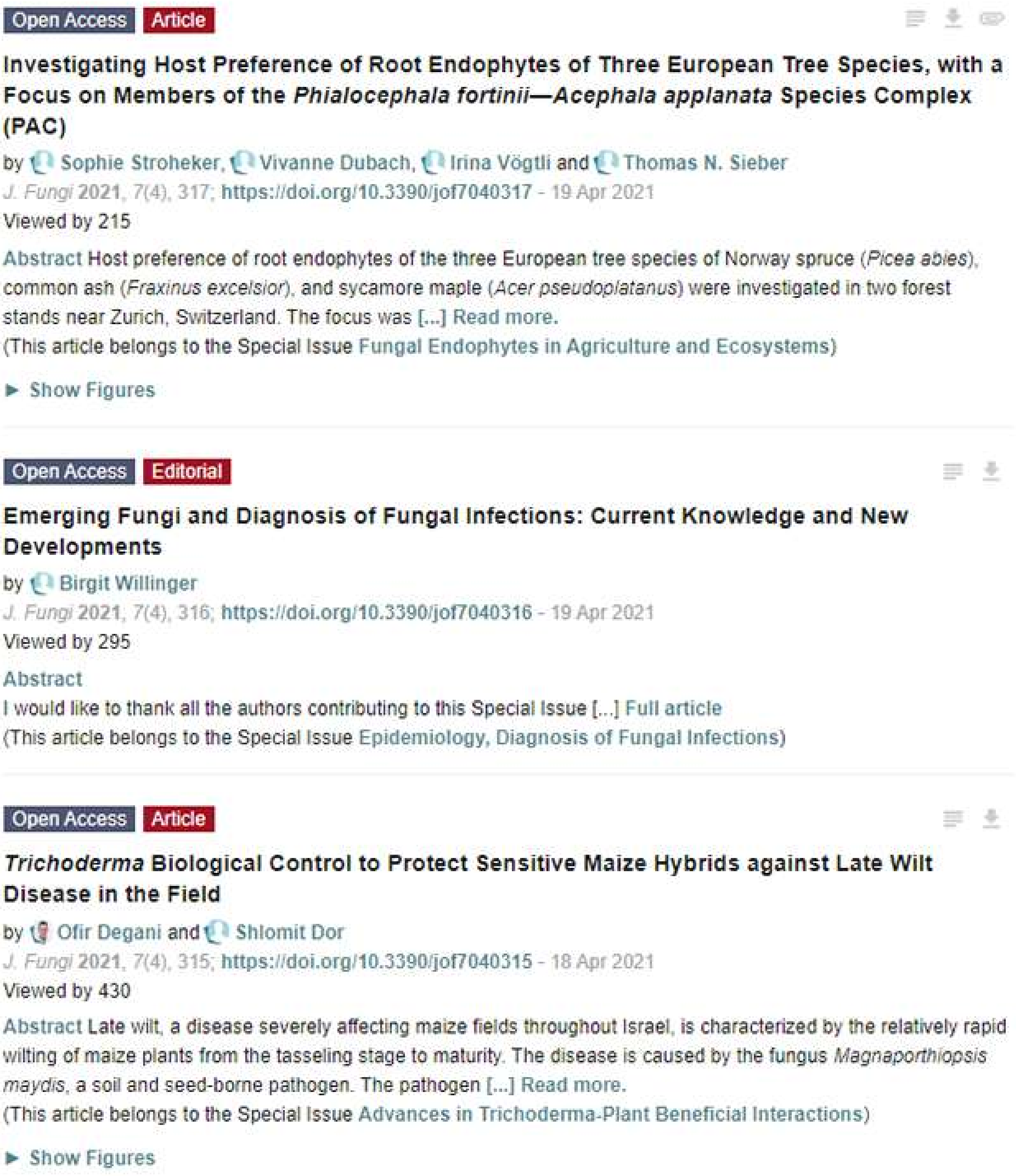

Open Access Article

Investigating Host Preference of Root Endophytes of Three European Tree Species, with a Focus on Members of the *Phialocephala fortinii—Acephala applanata* Species Complex (PAC)

by Sophie Stroheker, Vivanne Dubach, Irina Vögtli and Thomas N. Sieber

J. Fungi **2021**, *7*(4), 317; https://doi.org/10.3390/jof7040317 - 19 Apr 2021

Viewed by 215

Abstract Host preference of root endophytes of the three European tree species of Norway spruce (*Picea abies*), common ash (*Fraxinus excelsior*), and sycamore maple (*Acer pseudoplatanus*) were investigated in two forest stands near Zurich, Switzerland. The focus was [...] Read more.

(This article belongs to the Special Issue Fungal Endophytes in Agriculture and Ecosystems)

► Show Figures

Open Access Editorial

Emerging Fungi and Diagnosis of Fungal Infections: Current Knowledge and New Developments

by Birgit Willinger

J. Fungi **2021**, *7*(4), 316; https://doi.org/10.3390/jof7040316 - 19 Apr 2021

Viewed by 295

Abstract

I would like to thank all the authors contributing to this Special Issue [...] Full article

(This article belongs to the Special Issue Epidemiology, Diagnosis of Fungal Infections)

Open Access Article

Trichoderma Biological Control to Protect Sensitive Maize Hybrids against Late Wilt Disease in the Field

by Ofir Degani and Shlomit Dor

J. Fungi **2021**, *7*(4), 315; https://doi.org/10.3390/jof7040315 - 18 Apr 2021

Viewed by 430

Abstract Late wilt, a disease severely affecting maize fields throughout Israel, is characterized by the relatively rapid wilting of maize plants from the tasseling stage to maturity. The disease is caused by the fungus *Magnaporthiopsis maydis*, a soil and seed-borne pathogen. The pathogen [...] Read more.

(This article belongs to the Special Issue Advances in Trichoderma-Plant Beneficial Interactions)

► Show Figures

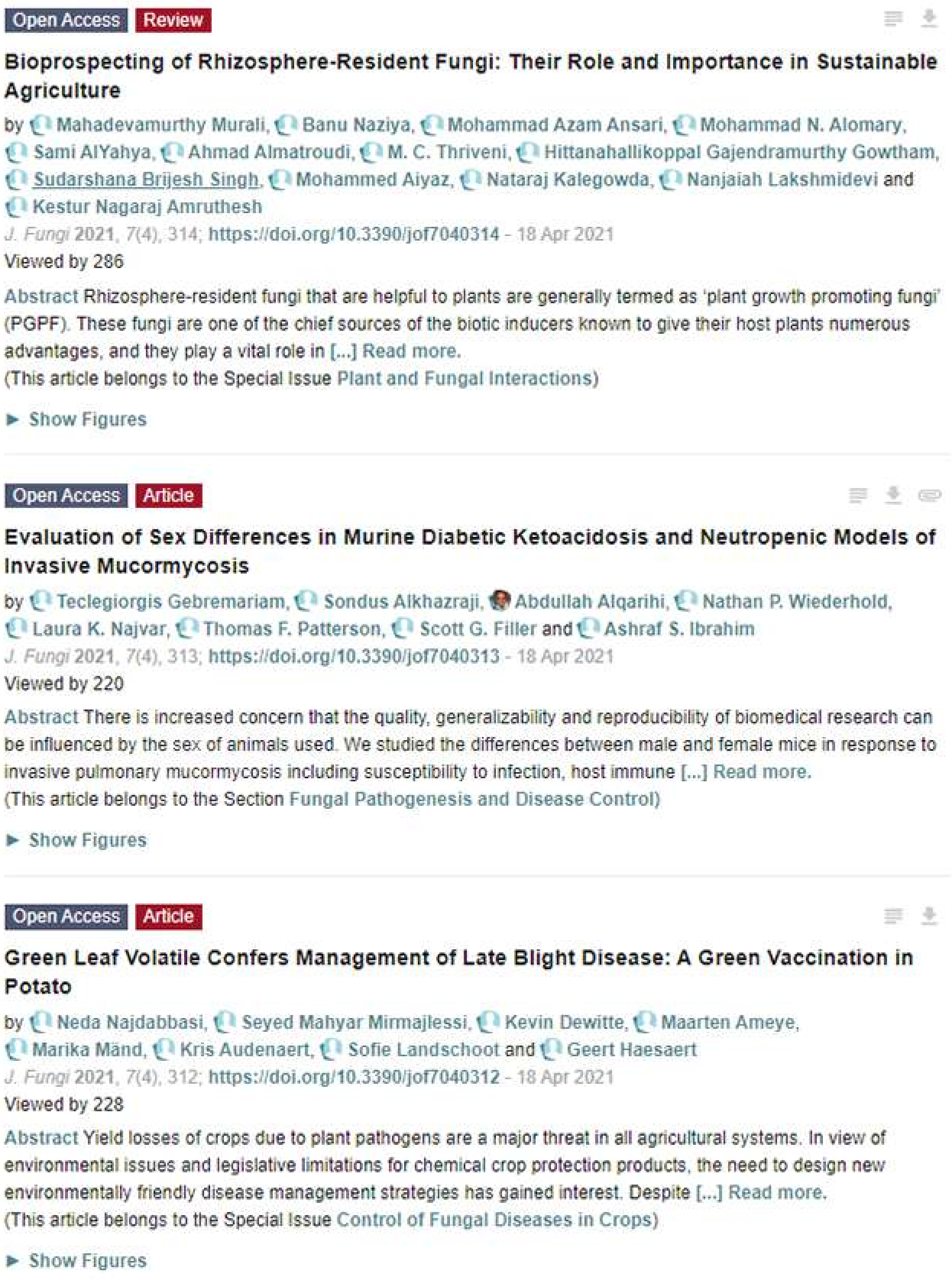

Open Access Review

Bioprospecting of Rhizosphere-Resident Fungi: Their Role and Importance in Sustainable Agriculture

by Mahadevamurthy Murali, Banu Naziya, Mohammad Azam Ansari, Mohammad N. Alomary, Sami AlYahya, Ahmad Almatroudi, M. C. Thriveni, Hittanahallikoppal Gajendramurthy Gowtham, Sudarshana Brijesh Singh, Mohammed Aiyaz, Nataraj Kalegowda, Nanjaiah Lakshmidevi and Kestur Nagaraj Amruthesh

J. Fungi **2021**, *7*(4), 314; https://doi.org/10.3390/jof7040314 - 18 Apr 2021

Viewed by 286

Abstract Rhizosphere-resident fungi that are helpful to plants are generally termed as 'plant growth promoting fungi' (PGPF). These fungi are one of the chief sources of the biotic inducers known to give their host plants numerous advantages, and they play a vital role in [...] Read more.

(This article belongs to the Special Issue Plant and Fungal Interactions)

► Show Figures

Open Access Article

Evaluation of Sex Differences in Murine Diabetic Ketoacidosis and Neutropenic Models of Invasive Mucormycosis

by Teclegiorgis Gebremariam, Sondus Alkhazraji, Abdullah Alqarihi, Nathan P. Wiederhold, Laura K. Najvar, Thomas F. Patterson, Scott G. Filler and Ashraf S. Ibrahim

J. Fungi **2021**, *7*(4), 313; https://doi.org/10.3390/jof7040313 - 18 Apr 2021

Viewed by 220

Abstract There is increased concern that the quality, generalizability and reproducibility of biomedical research can be influenced by the sex of animals used. We studied the differences between male and female mice in response to invasive pulmonary mucormycosis including susceptibility to infection, host immune [...] Read more.

(This article belongs to the Section Fungal Pathogenesis and Disease Control)

► Show Figures

Open Access Article

Green Leaf Volatile Confers Management of Late Blight Disease: A Green Vaccination in Potato

by Neda Najdabbasi, Seyed Mahyar Mirmajlessi, Kevin Dewitte, Maarten Ameye, Marika Mänd, Kris Audenaert, Sofie Landschoot and Geert Haesaert

J. Fungi **2021**, *7*(4), 312; https://doi.org/10.3390/jof7040312 - 18 Apr 2021

Viewed by 228

Abstract Yield losses of crops due to plant pathogens are a major threat in all agricultural systems. In view of environmental issues and legislative limitations for chemical crop protection products, the need to design new environmentally friendly disease management strategies has gained interest. Despite [...] Read more.

(This article belongs to the Special Issue Control of Fungal Diseases in Crops)

► Show Figures

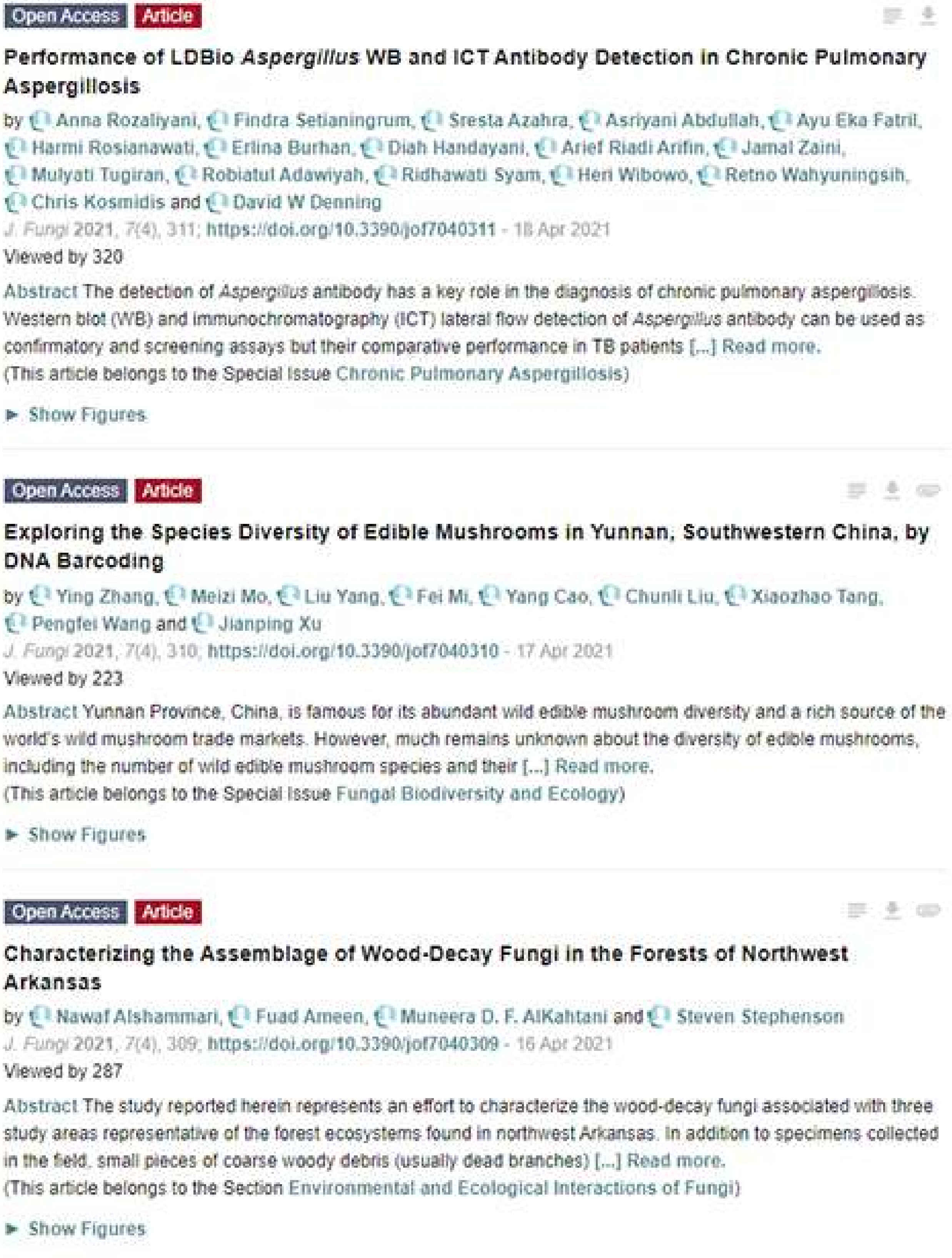

Performance of LDBio *Aspergillus* WB and ICT Antibody Detection in Chronic Pulmonary Aspergillosis

by Anna Rozaliyani, Findra Setianingrum, Sresta Azahra, Asriyani Abdullah, Ayu Eka Fatril, Harmi Rosianawati, Erlina Burhan, Diah Handayani, Arief Riadi Arifin, Jamal Zaini, Mulyati Tugiran, Robiatul Adawiyah, Ridhawati Syam, Heri Wibowo, Retno Wahyuningsih, Chris Kosmidis and David W Denning

J. Fungi 2021, *7*(4), 311; https://doi.org/10.3390/jof7040311 - 18 Apr 2021

Viewed by 320

Abstract The detection of *Aspergillus* antibody has a key role in the diagnosis of chronic pulmonary aspergillosis. Western blot (WB) and immunochromatography (ICT) lateral flow detection of *Aspergillus* antibody can be used as confirmatory and screening assays but their comparative performance in TB patients [...] Read more.

(This article belongs to the Special Issue Chronic Pulmonary Aspergillosis)

Exploring the Species Diversity of Edible Mushrooms in Yunnan, Southwestern China, by DNA Barcoding

by Ying Zhang, Meizi Mo, Liu Yang, Fei Mi, Yang Cao, Chunli Liu, Xiaozhao Tang, Pengfei Wang and Jianping Xu

J. Fungi 2021, *7*(4), 310; https://doi.org/10.3390/jof7040310 - 17 Apr 2021

Viewed by 223

Abstract Yunnan Province, China, is famous for its abundant wild edible mushroom diversity and a rich source of the world's wild mushroom trade markets. However, much remains unknown about the diversity of edible mushrooms, including the number of wild edible mushroom species and their [...] Read more.

(This article belongs to the Special Issue Fungal Biodiversity and Ecology)

Characterizing the Assemblage of Wood-Decay Fungi in the Forests of Northwest Arkansas

by Nawaf Alshammari, Fuad Ameen, Muneera D. F. AlKahtani and Steven Stephenson

J. Fungi 2021, *7*(4), 309; https://doi.org/10.3390/jof7040309 - 16 Apr 2021

Viewed by 287

Abstract The study reported herein represents an effort to characterize the wood-decay fungi associated with three study areas representative of the forest ecosystems found in northwest Arkansas. In addition to specimens collected in the field, small pieces of coarse woody debris (usually dead branches) [...] Read more.

(This article belongs to the Section Environmental and Ecological Interactions of Fungi)

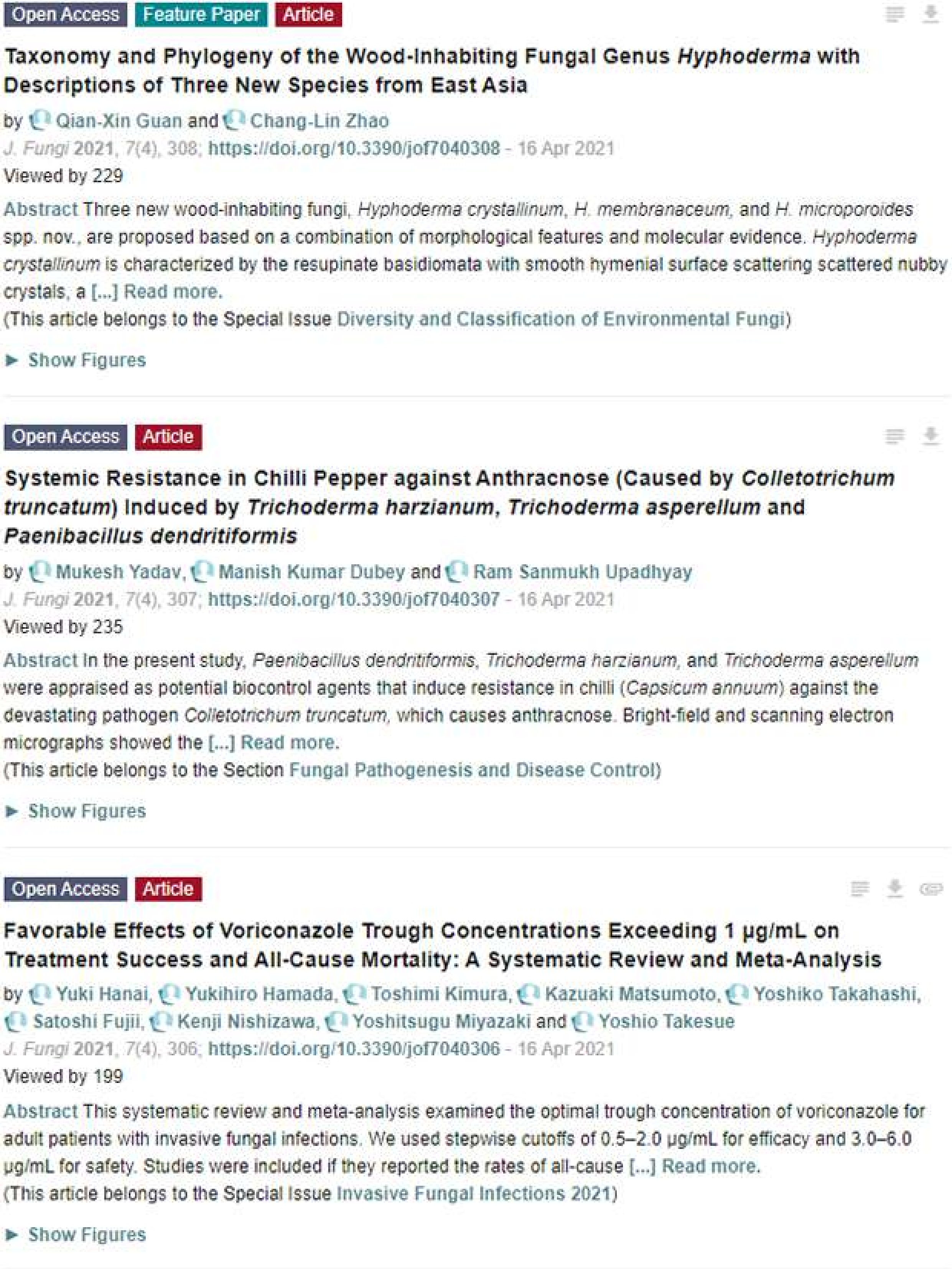

Open Access Feature Paper Article

Taxonomy and Phylogeny of the Wood-Inhabiting Fungal Genus *Hyphoderma* with Descriptions of Three New Species from East Asia

by Qian-Xin Guan and Chang-Lin Zhao

J. Fungi **2021**, 7(4), 308; **https://doi.org/10.3390/jof7040308** - 16 Apr 2021

Viewed by 229

Abstract Three new wood-inhabiting fungi, *Hyphoderma crystallinum*, *H. membranaceum*, and *H. microporoides* spp. nov., are proposed based on a combination of morphological features and molecular evidence. *Hyphoderma crystallinum* is characterized by the resupinate basidiomata with smooth hymenial surface scattering scattered nubby crystals, a [...] Read more.

(This article belongs to the Special Issue Diversity and Classification of Environmental Fungi)

▶ Show Figures

Open Access Article

Systemic Resistance in Chilli Pepper against Anthracnose (Caused by *Colletotrichum truncatum*) Induced by *Trichoderma harzianum*, *Trichoderma asperellum* and *Paenibacillus dendritiformis*

by Mukesh Yadav, Manish Kumar Dubey and Ram Sanmukh Upadhyay

J. Fungi **2021**, 7(4), 307; **https://doi.org/10.3390/jof7040307** - 16 Apr 2021

Viewed by 235

Abstract In the present study, *Paenibacillus dendritiformis*, *Trichoderma harzianum*, and *Trichoderma asperellum* were appraised as potential biocontrol agents that induce resistance in chilli (*Capsicum annuum*) against the devastating pathogen *Colletotrichum truncatum*, which causes anthracnose. Bright-field and scanning electron micrographs showed the [...] Read more.

(This article belongs to the Section Fungal Pathogenesis and Disease Control)

▶ Show Figures

Open Access Article

Favorable Effects of Voriconazole Trough Concentrations Exceeding 1 μg/mL on Treatment Success and All-Cause Mortality: A Systematic Review and Meta-Analysis

by Yuki Hanai, Yukihiro Hamada, Toshimi Kimura, Kazuaki Matsumoto, Yoshiko Takahashi, Satoshi Fujii, Kenji Nishizawa, Yoshitsugu Miyazaki and Yoshio Takesue

J. Fungi **2021**, 7(4), 306; **https://doi.org/10.3390/jof7040306** - 16 Apr 2021

Viewed by 199

Abstract This systematic review and meta-analysis examined the optimal trough concentration of voriconazole for adult patients with invasive fungal infections. We used stepwise cutoffs of 0.5–2.0 μg/mL for efficacy and 3.0–6.0 μg/mL for safety. Studies were included if they reported the rates of all-cause [...] Read more.

(This article belongs to the Special Issue Invasive Fungal Infections 2021)

▶ Show Figures

Journal of
Fungi

Article

Taxonomy and Phylogeny of the Wood-Inhabiting Fungal Genus *Hyphoderma* with Descriptions of Three New Species from East Asia

Qian-Xin Guan [1,2] and Chang-Lin Zhao [1,2,*]

[1] Key Laboratory for Forest Resources Conservation and Utilization in the Southwest Mountains of China, Ministry of Education, Southwest Forestry University, Kunming 650224, China; zongtongkai@im.ac.cn
[2] College of Biodiversity Conservation, Southwest Forestry University, Kunming 650224, China
* Correspondence: fungi@swfu.edu.cn or fungichanglinz@163.com

Abstract: Three new wood-inhabiting fungi, *Hyphoderma crystallinum*, *H. membranaceum*, and *H. microporoides* spp. nov., are proposed based on a combination of morphological features and molecular evidence. *Hyphoderma crystallinum* is characterized by the resupinate basidiomata with smooth hymenial surface scattering scattered nubby crystals, a monomitic hyphal system with clamped generative hyphae, and numerous encrusted cystidia present. *Hyphoderma membranaceum* is characterized by the resupinate basidiomata with tuberculate hymenial surface, presence of the moniliform cystidia, and ellipsoid to cylindrical basidiospores. *Hyphoderma microporoides* is characterized by the resupinate, cottony basidiomata distributing the scattered pinholes visible using hand lens on the hymenial surface, presence of halocystidia, and cylindrical to allantoid basidiospores. Sequences of ITS+nLSU rRNA gene regions of the studied samples were generated, and phylogenetic analyses were performed with maximum likelihood, maximum parsimony, and Bayesian inference methods. These phylogenetic analyses showed that three new species clustered into *Hyphoderma*, in which *H. crystallinum* was sister to *H. variolosum*, *H. membranaceum* was retrieved as a sister species of *H. sinense*, and *H. microporoides* was closely grouped with *H. nemorale*. In addition to new species, map to show global distribution of *Hyphoderma* species treated in the phylogenetic tree and an identification key to Chinese *Hyphoderma* are provided.

Keywords: corticioid fungi; *Hyphoderma*; hyphodermataceae; molecular systematics; Yunnan Province

check for updates

Citation: Guan, Q.-X.; Zhao, C.-L. Taxonomy and Phylogeny of the Wood-Inhabiting Fungal Genus *Hyphoderma* with Descriptions of Three New Species from East Asia. *J. Fungi* **2021**, *7*, 308. https://doi.org/10.3390/jof7040308

Academic Editors: Samantha C. Karunarathna and Saowaluck Tibpromma

Received: 28 March 2021
Accepted: 15 April 2021
Published: 16 April 2021

1. Introduction

Fungi are an ecologically important branch of the tree of life based on its distinct and diverse characteristics, in which these organisms play a vital role in ecosystems as diverse as soil, forest, rocks, and ocean, but their roles are primarily enacted behind the scenes, literally as hidden layers within their substrate [1]. On the basis of the nature of their intertwined partners in numerous symbiotic interactions, they have mostly marched via stepwise codiversification with the plants [2]. Fungi have evolved numerous strategies to degrade hard-to-digest substrates for outcompeting with other microbes, while combating competitors using an arsenal of bioactive metabolites, such as the familiar antibiotics, ethanol, and organic acids [3]. Taxonomy plays a central role in understanding the diversity of life, discovering into systems of names that capture the relationships between species, and translating the products of biological exploration [4]. Despite the early embrace of the molecular systematics by mycologists, both the discovery and classification of fungi are still in great flux, particularly among the more basal branches of the tree, in which the true diversity is only now coming to light from genomic analyses and environmental DNA surveys [1]. The researches revealed that perhaps less than 5% of the estimated two to four million species have been formally described, therefore, the hidden and microscopic nature of many fungi also means that their diversity is undersampled [5,6].

The genus *Hyphoderma* Wallr. is one of the most important fungal groups because of its key role in the carbon cycle and being the most efficient wood decomposers in the forest ecosystem [7]. This genus is typified by *H. setigerum* (Fr.) Donk [8]. *Hyphoderma* is characterized by the resupinate to effuse-reflexed basidiomata with ceraceous consistency, and smooth to tuberculate or hydnoid hymenophore and a monomitic hyphal structure (rarely dimitic) with clamp connections on generative hyphae, presence of cystidia or not, basidia suburniform to subcylindrical and cylindrical, ellipsoid to subglobose, smooth, thin-walled basidiospores [9,10]. Currently, about 100 species have been accepted in *Hyphoderma* worldwide [8,11–15]. Index Fungorum (http://www.indexfungorum.org; accessed on 16 April 2021) and MycoBank (https://www.mycobank.org; accessed on 16 April 2021) register 192 specific and infraspecific names in *Hyphoderma*.

Molecular systematics covering *Hyphoderma* revealed the classification of corticioid fungi and showed that *H. obtusum* J. Erikss. and *H. setigerum* clustered into Meruliaceae Rea and then grouped with *Hypochnicium polonense* (Bres.) Å. Strid, based on the internal transcribed spacer (ITS) regions and the large subunit nuclear ribosomal RNA gene (nLSU) sequences [16]. Telleria et al. [17] discussed the relationships between *Hyphoderma* and *Peniophorella* P. Karst., in which some species from *Hyphoderma* and *Peniophorella* are grouped and they proposed a new species, *H. macaronesicum* Tellería et al. The research on studying *Hyphoderma setigerum* complex showed that *H. pinicola* Yurch. and Sheng H. Wu represented a fifth species in this complex, which revealed that this complex was a white-rot wood-decaying corticoid fungal species and occurred worldwide from tropical to temperate regions [18]. A revised family-level classification of the Polyporales revealed that four *Hyphoderma* species nested into the residual polyporoid clade belonging to Hyphodermataceae, and then, they were grouped with three related genera *Meripilus* P. Karst., *Physisporinus* P. Karst., and *Rigidoporus* Murrill [19]. Chinese *Hyphoderma* species were compared with closely related taxa, and two new species were proposed, *H. fissuratum* C.L. Zhao and X. Ma and *H. mopanshanense* C.L. Zhao [15].

In this study, three undescribed species of corticioid fungi were collected from Yunnan Province, China. Morphological characteristics and molecular phylogenetic analyses of combined ITS+nLSU rRNA sequences supported the recognition of three new species within *Hyphoderma*.

2. Materials and Methods

2.1. Morphology

The studied specimens are deposited at the herbarium of Southwest Forestry University (SWFC), Kunming, Yunnan Province, China. Macromorphological descriptions are based on field notes and photos captured in the field and laboratory. Color terminology follows Petersen [20]. Micromorphological data were obtained from the dried specimens, which were observed under a light microscope following Dai [21]. The following abbreviations are used: KOH = 5% potassium hydroxide water solution, CB = Cotton Blue, CB– = acyanophilous, IKI = Melzer's reagent, IKI– = both inamyloid and indextrinoid, L = mean spore length (arithmetic average for all spores), W = mean spore width (arithmetic average for all spores), Q = variation in the L/W ratios between the specimens studied, n = a/b (number of spores (a) measured from given number (b) of specimens).

2.2. Molecular Phylogeny

CTAB rapid plant genome extraction kit-DN14 (Aidlab Biotechnologies Co., Ltd., Beijing, China) was used to obtain genomic DNA from dried specimens, according to the manufacturer's instructions [22]. ITS region was amplified with primer pair ITS5 and ITS4 [23]. Nuclear nLSU region was amplified with primer pair LR0R and LR7 (http://lutzonilab.org/nuclear-ribosomal-dna/; accessed on 16 April 2021). The PCR procedure for ITS was as follows: initial denaturation at 95 °C for 3 min; followed by 35 cycles at 94 °C for 40 s, 58 °C for 45 s, and 72 °C for 1 min; and a final extension of 72 °C for 10 min. The PCR procedure for nLSU was as follows: initial denaturation at 94 °C for 1 min; followed by 35 cycles at 94 °C for 30 s, 48 °C for 1 min, and 72 °C for 1.5 min; and a final extension of 72 °C for 10 min. The PCR products were purified and directly sequenced at Kunming Tsingke Biological Technology Limited Company, Kunming, Yunnan Province, China. All newly generated sequences were deposited in NCBI GenBank (Table 1).

Table 1. List of species, specimens, and GenBank accession numbers of sequences used in this study.

Species Name	Specimen No.	GenBank Accession No.		References
		ITS	LSU	
Climacocystis borealis	FD-31	KP135308	KP135210	[19]
Diplomitoporus crustulinus	FD-137	KP135299	KP135211	[19]
Hyphoderma amoenum	USO 286622	HE577030		[17]
H. assimile	CBS 125852	MH863808	MH875272	[24]
H. cremeoalbum	NH 11538	DQ677492	DQ677492	[16]
H. crystallinum	**CLZhao 9338**	**MW917161**	**MW913414**	**Present study**
H. crystallinum	**CLZhao 9374**	**MW917162**	**MW913415**	**Present study**
H. crystallinum	**CLZhao 10224**	**MW917163**	**MW913416**	**Present study**
H. crystallinum	**CLZhao 11723**	**MW917164**	**MW913417**	**Present study**
H. crystallinum	**CLZhao 15841**	**MW917165**	**MW913418**	**Present study**
H. crystallinum	**CLZhao 18459**	**MW917166**	**MW913419**	**Present study**
H. definitum	GEL 2898		AJ406509	[18]
H. definitum	NH 12266	DQ677493	DQ677493	[16]
H.fissuratum	CLZhao 6731	MT791331	MT791335	[15]
H.fissuratum	CLZhao 6726	MT791330	MT791334	[15]
H. floccosum	CLZhao 17129	MW301683	MW293733	[25]
H. floccosum	CLZhao 17296	MW301686	MW293736	[25]
H. floccosum	CLZhao 16492	MW301688	MW293734	[25]
H. floccosum	CLZhao 17215	MW301687	MW293735	[25]
H. floccosum	CLZhao 17079	MW301685		[25]
H. floccosum	CLZhao 17065	MW301684		[25]
H. granuliferum	KHL 12561	JN710545	JN710545	[18]
H. incrustatum	KHL 6685		AY586668	[18]
H. litschaueri	NH 7603	DQ677496	DQ677496	[16]
H. litschaueri	FP-101740- sp	KP135295	KP135219	[26]
H. macaronesicum	MA:Fungi:16099	HE577027		[18]
H. macaronesicum	TFC:Mic.15981	HE577028		[18]
H. medioburiense	NH 10950	DQ677497	DQ677497	[16]
H. membranaceum	**CLZhao 5844**	**MW917167**	**MW913420**	**Present study**
H. membranaceum	**CLZhao 6971**	**MW917168**	**MW913421**	**Present study**
H. microporoides	**CLZhao 6857**	**MW917169**	**MW913422**	**Present study**
H. microporoides	**CLZhao 8695**	**MW917170**	**MW913423**	**Present study**
H. moniliforme	Wu 0211-42	KC928282	KC928283	[27]
H. moniliforme	Wu 0211-46	KC928284	KC928285	[27]
H. mopanshanense	CLZhao 6498	MT791329	MT791333	[15]
H. mopanshanense	CLZhao 6493	MT791328	MT791332	[15]
H. nemorale	TNM F3931	KJ885183	KJ885184	[27]
H. nemorale	Wu 9508-14	KC928280	KC928281	[27]
H. nudicephalum	Wu 9307-29	AJ534269		[28]
H. nudicephalum	Wu 9508-225	AJ534268		[28]
H. obtusiforme	KHL 1464	JN572909		[29]
H. obtusiforme	KHL 11105	JN572910		[29]
H. obtusum	JS 17804		AY586670	[29]
H. occidentale	KHL 8469		AY586674	[29]
H. occidentale	KHL 8477	DQ677499	DQ677499	[16]
H. paramacaronesicum	MA:Fungi:87736	KC984399	KF150074	[14]
H. paramacaronesicum	MA:Fungi:87737	KC984405	KF150073	[14]
H. pinicola	Wu 0108-32	KJ885181	KJ885182	[29]
H. pinicola	Wu 0108-36	KC928278	KC928279	[29]
H. prosopidis	E09/58-9	HE577029		[29]
H. roseocremeum	NH 10545		AY586672	[29]

Table 1. *Cont.*

Species Name	Specimen No.	GenBank Accession No.		References
		ITS	LSU	
H. variolosum	CBS 734.91	MH862320	MH873992	[24]
H. variolosum	CBS 735.91	MH862321	MH873993	[24]
Hypochnicium cremicolor	CBS 208.54	MH857294	MH868826	[24]
H. erikssonii	NH 9635	DQ677508	DQ677508	[16]
H. geogenium	NH 10910	DQ677509	DQ677509	[16]
H. geogenium	MA-Fungi 48308	FN552534	JN939576	[30]
H. michelii	MA-Fungi 79155	NR119742	NG060635	[30]
H. punctulatum	FP101698sp	KY948827	KY948860	[19]
H. sphaerosporum	RLG15138sp	KY948803	KY948861	[19]
H. wakefieldiae	MA-Fungi 7675	FN552531	JN939577	[30]
Physisporinus subcrocatus	Dai 15917	KY131870	KY131926	[31]
P. subcrocatus	Dai 12800	KY131869	KY131925	[31]
P. tibeticus	Cui 9588	KY131873	KY131929	[31]
P. tibeticus	Cui 9518	KY131872	KY131928	[31]
Rigidoporus eminens	Dai 17200	MT279690	MT279911	[31]
R. undatus	Miettinen-13591	KY948731	KY948870	[19]

New sequences are shown in bold.

Sequences were aligned in MAFFT 7 (https://mafft.cbrc.jp/alignment/server/; accessed on 10 April 2021) using the "G-INS-i" strategy for ITS+nLSU and manually adjusted in BioEdit [32]. The dataset was aligned first and then, ITS and nLSU sequences were combined with Mesquite. Alignment datasets were deposited in TreeBASE (submission ID 27983). *Climacocystis borealis* (Fr.) Kotl. and Pouzar and *Diplomitoporus crustulinus* (Bres.) Domański were selected as an outgroup for phylogenetic analysis of ITS+nLSU phylogenetic tree (Figure 1) following a previous study [19].

Maximum parsimony analysis was applied to the combined (ITS+nLSU) dataset. Its approaches followed previous study [22], and the tree construction procedure was performed in PAUP* version 4.0b10 [33]. All characters were equally weighted and gaps were treated as missing data. Trees were inferred using the heuristic search option with TBR branch swapping and 1000 random sequence additions. Max-trees were set to 5000, branches of zero length were collapsed, and all parsimonious trees were saved. Clade robustness was assessed using bootstrap (BT) analysis with 1000 replicates [34]. Descriptive tree statistics: tree length (TL), consistency index (CI), retention index (RI), rescaled consistency index (RC), and homoplasy index (HI) were calculated for each maximum parsimonious tree generated. Datamatrix was also analyzed using maximum likelihood (ML) approach with RAxML-HPC2 through the CIPRES Science Gateway (www.phylo.org; accessed on 8 April 2021) [35]. Branch support (BS) for ML analysis was determined by 1000 bootstrap replicates.

MrModeltest 2.3 [36] was used to determine the best-fit evolution model for each data set for Bayesian inference (BI). BI was calculated with MrBayes 3.1.2 [37]. Four Markov chains were run for 2 runs from random starting trees for 6 million generations for ITS+nLSU (Figure 1). The first one-fourth of all generations was discarded as burn-in. The majority rule consensus tree of all remaining trees was calculated. Branches were considered as significantly supported if they received maximum likelihood bootstrap value (BS) > 70%, maximum parsimony bootstrap value (BT) > 70%, or Bayesian posterior probabilities (BPP) > 0.95.

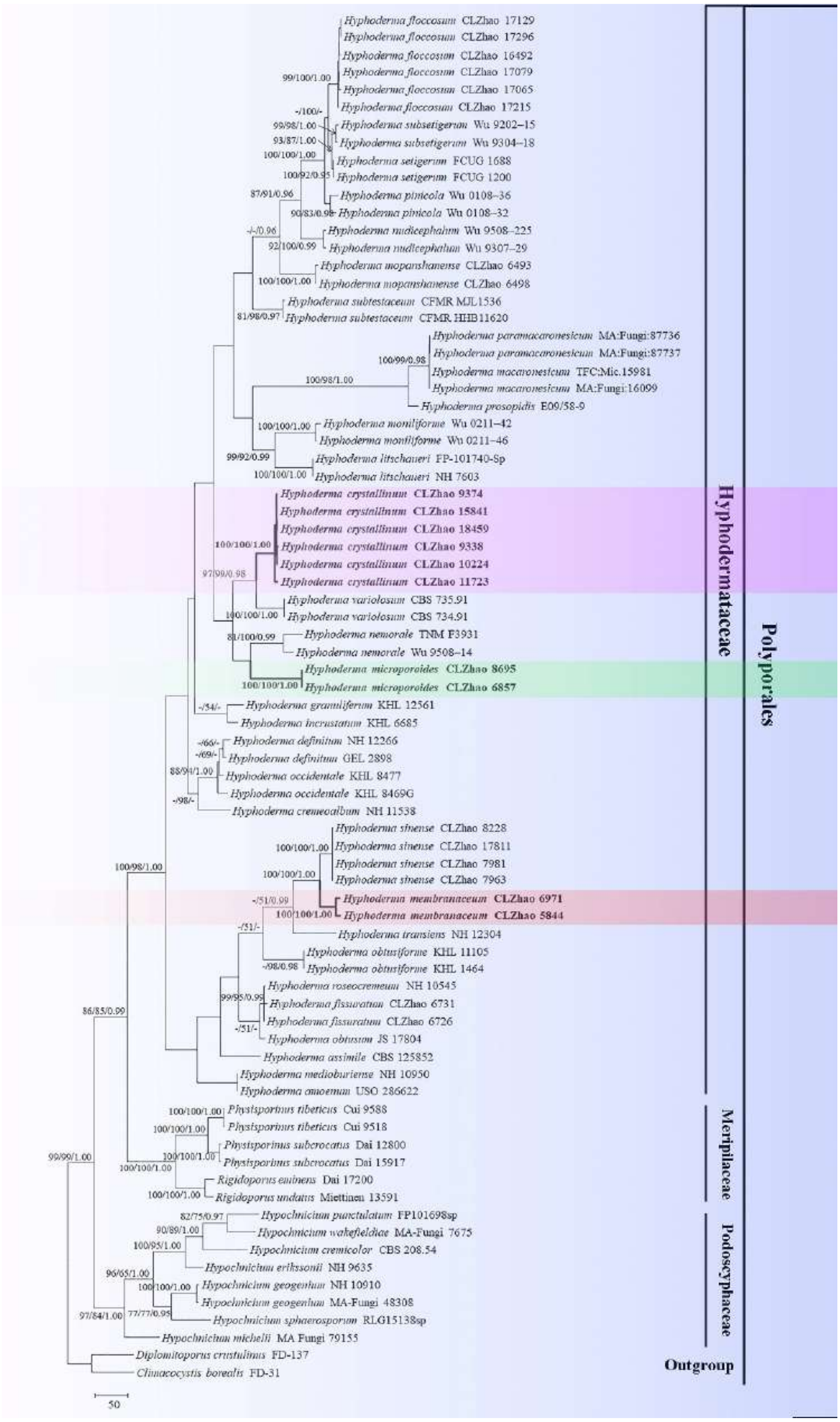

Figure 1. Maximum Parsimony strict consensus tree illustrating the phylogeny of three new species and related species in *Hyphoderma* within Polyporales based on internal transcribed spacer + nuclear ribosomal RNA gene (ITS+nLSU) sequences. Branches are labeled with maximum likelihood bootstrap values > 70%, parsimony bootstrap values > 50% and Bayesian posterior probabilities > 0.95. The new species are in bold. Clade names follow previous study [19].

3. Results

3.1. Molecular Phylogeny

The ITS+nLSU dataset (Figure 1) included sequences from 78 fungal specimens representing 44 taxa. The dataset had an aligned length of 2086 characters, of which 1245 characters are constant, 127 are variable and parsimony-uninformative, and 714 are parsimony-informative. Maximum parsimony analysis yielded 5000 equally parsimonious trees (TL = 3441, CI = 0.3787, HI = 0.6213, RI = 0.7178, RC = 0.2718). Best model for the ITS+nLSU dataset estimated and applied in the Bayesian analysis was GTR+I+G (lset nst = 6, rates = invgamma; prset statefreqpr = dirichlet (1,1,1,1)). Bayesian analysis and ML analysis resulted in a similar topology to MP analysis with an average standard deviation of split frequencies = 0.007698 (BI).

The phylogram inferred from ITS+nLSU sequences (Figure 1) demonstrated that three new species are clustered into genus *Hyphoderma*, in which *H. crystallinum* was sister to *H. variolosum* Boidin, Lanq. and Gilles, *H. membranaceum* was retrieved as a sister species of *H. sinense* C.L. Zhao and Q.X. Guan, and *H. microporoides* was closely grouped with *H. nemorale* K.H. Larss. (100% BS, 100% BP, and 1.00 BPP).

3.2. Taxonomy

Hyphoderma crystallinum C.L. Zhao and Q.X. Guan, sp. nov. Figures 2 and 3.

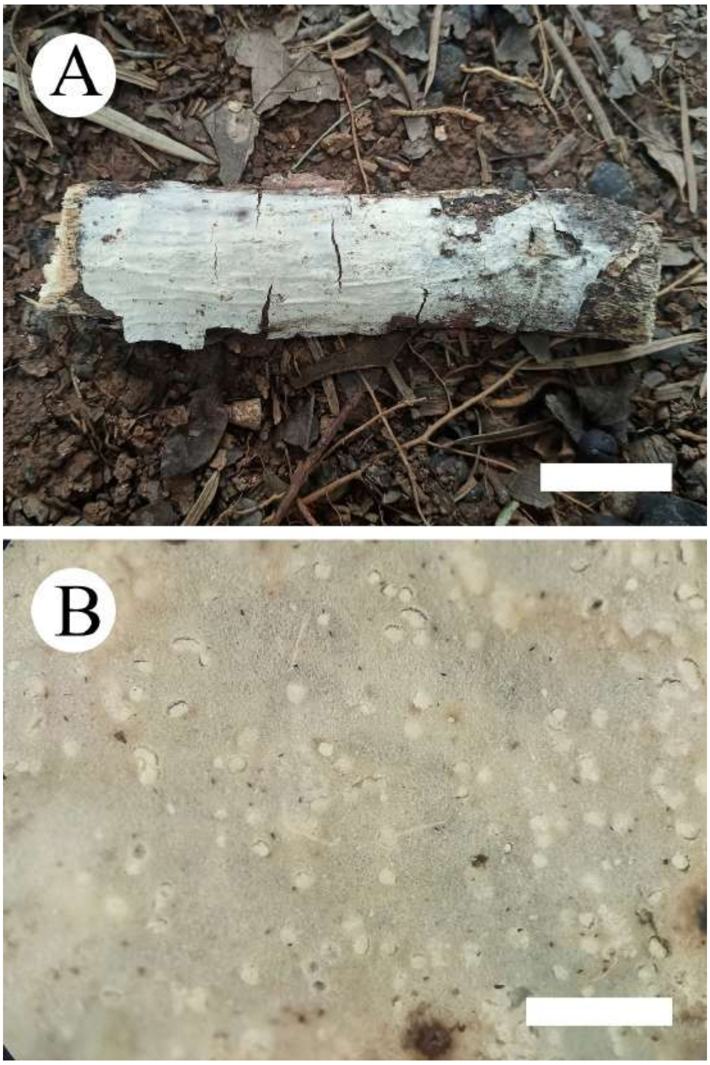

Figure 2. *Hyphoderma crystallinum* (holotype) (**A**): basidiomata on the substrate (**B**); scattered nubby crystals. Bars: **A** = 2 cm and **B** = 1 mm.

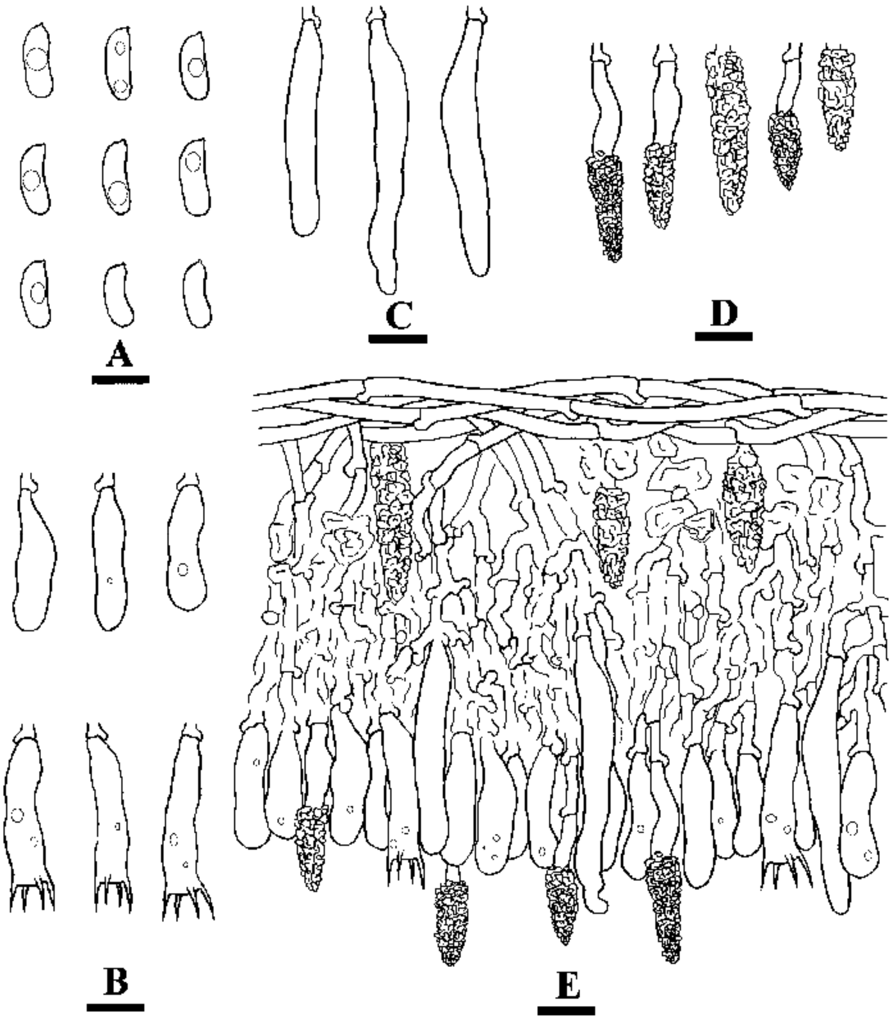

Figure 3. Microscopic structures of *Hyphoderma crystallinum* (holotype) (**A**): basidiospores (**B**), basidia and basidioles (**C**), tubular cystidia (**D**), and encrusted cystidia (**E**). A section of hymenium. Bars: **A**–**E** = 10 µm.

MycoBank no.: MB 839276.

Holotype—China, Yunnan Province, Puer, Jingdong County, the Forest of Pineapple, E 100°48′, N 24°21′, 2113 m asl., on fallen angiosperm branch, leg. C.L. Zhao, 4 January 2019, C.L. Zhao 9338 (SWFC).

Etymology—***crystallinum*** (Lat.): referring to the numerous and larger crystals on the hymenial surface.

Fruiting body—Basidiomata annual, resupinate, adnate, without odor and taste when fresh, membranaceous when fresh, becoming hard membranaceous upon drying, and up to 15 cm long, 3 cm wide, and 30–100 µm thick. Hymenial surface white to pale gray when fresh, pale gray to slightly cream upon drying, with scattered nubby crystals. Margin sterile indistinct and white.

Hyphal system—Monomitic, generative hyphae with clamp connections, colorless, thin-walled, frequently branched, interwoven, 2–3.5 µm in diameter, IKI-, CB-; tissues unchanged in KOH.

Hymenium—Cystidia of two types: (1) tubular cystidia, colorless, thin-walled, 32–51 µm × 5–10 µm and (2) encrusted cystidia, numerous, colorless, encrusted by crystals, 14–46 µm × 4–11 µm. Basidia clavate to subcylindrical, slightly constricted in the middle to somewhat sinuous, with 4 sterigmata and a basal clamp connection, 21.5–31 µm × 6–8.5 µm.

Spores—Basidiospores allantoid, colorless, thin-walled, smooth, with oil drops inside, IKI-, CB-, (10.5–)11–14.5(–15) µm × 4–5.5(–6) µm, L = 12.99 µm, W = 4.81 µm, Q = 2.47–2.98 (n = 90/3).

Additional specimens examined—China, Yunnan Province, Puer, Jingdong County, the Forest of Pineapple, E 100°48′, N 24°21′, 2113 m asl., on fallen angiosperm branch, leg. C.L. Zhao, 4 January 2019, C.L. Zhao 9374 (SWFC); Dali, Nanjian County, Lingbaoshan National Forestry Park, E 100°30′, N 24°46′, 1963 m asl., on fallen angiosperm branch, leg. C.L. Zhao, 9 January 2019, C.L. Zhao 10224 (SWFC); Wenshan, Funing County, Guying village, E 105°35′, N 23°36′, 976 m asl., on fallen angiosperm branch, leg. C.L. Zhao, 20 January 2019, C.L. Zhao 11723 (SWFC); Wenshan, Xichou County, Jiguanshan Forestry Park, E 103°46′, N 23°33′, 1670 m asl., on fallen angiosperm trunk, leg. C.L. Zhao, 22 July 2019, C.L. Zhao 15841 (SWFC); Honghe, Pingbian County, Daweishan National Nature Reserve, E 103°35′, N 22°53′, 1990 m asl., on fallen angiosperm branch, leg. C.L. Zhao, 3 August 2019, C.L. Zhao 18459 (SWFC).

Hyphoderma membranaceum C.L. Zhao and Q.X. Guan sp. nov. Figures 4 and 5.

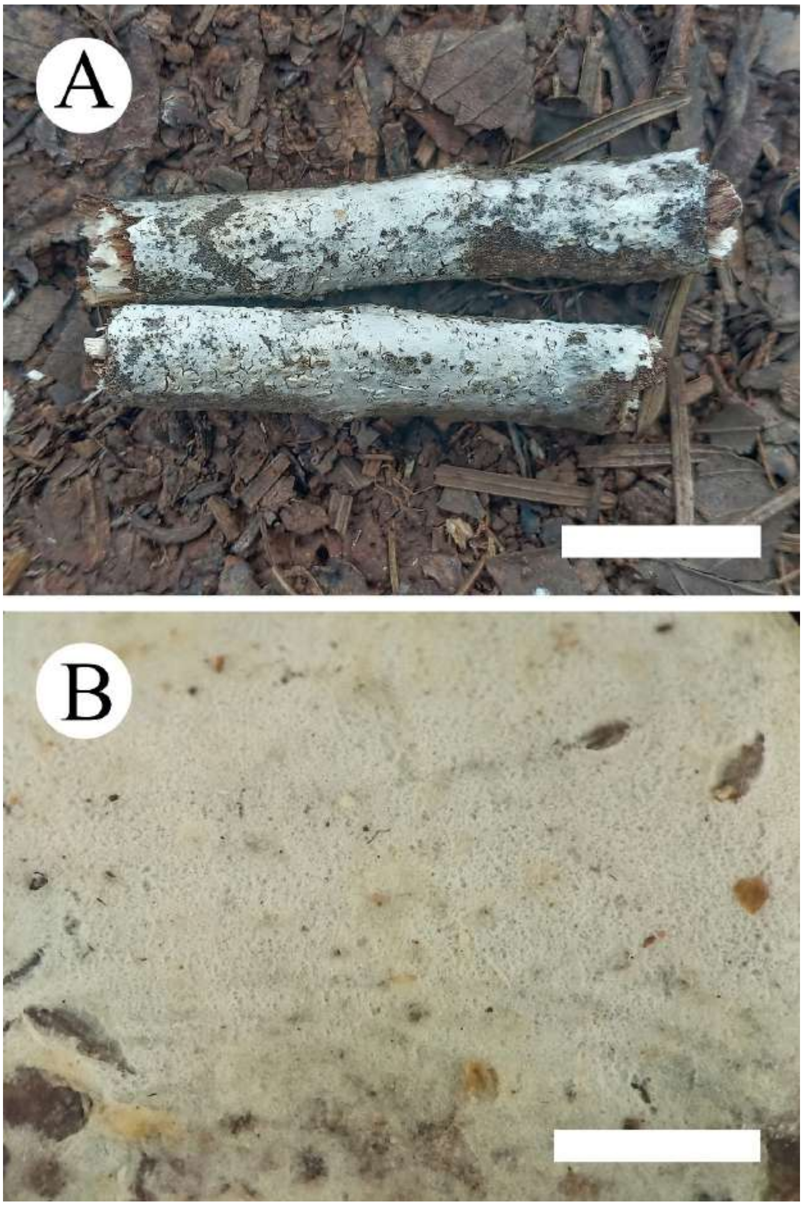

Figure 4. Basidiomata (**A**) of *Hyphoderma membranaceum* (**B**) (holotype). Bars: **A** = 2 cm and **B** = 1 mm.

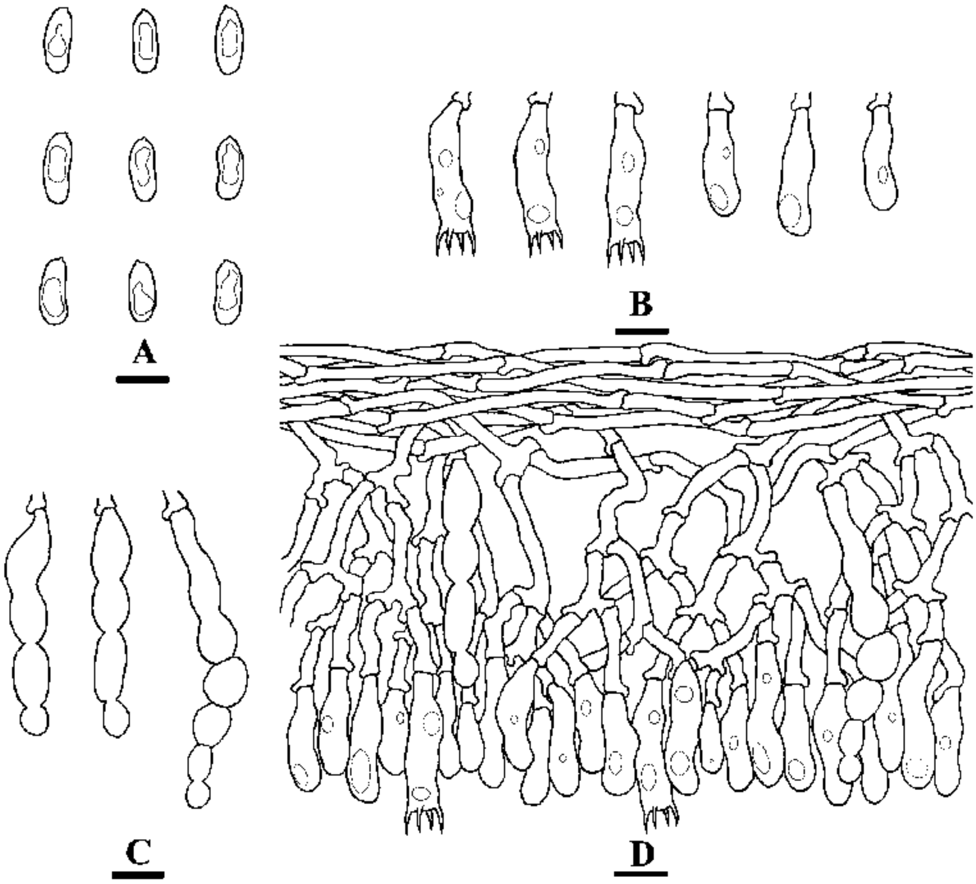

Figure 5. Microscopic structures of *Hyphoderma membranaceum* (holotype) (**A**): basidiospores (**B**), basidia and basidioles (**C**), and cystidia (**D**). A section of hymenium. Bars: **A**–**D** = 10 µm.

MycoBank no.: MB 839278.

Holotype—China, Yunnan Province, Chuxiong, Zixishan Forestry Park, E 101°24′, N 25°01′, 2356 m asl., on fallen angiosperm branch, leg. C.L. Zhao, 1 July 2018, C.L. Zhao 6971 (SWFC).

Etymology—*membranaceum* (Lat.): referring to the membranous hymenophore.

Fruiting body—Basidiomata annual, resupinate, adnate, membranous, without odor and taste when fresh, and up to 15 cm long, 2 cm wide, and 30–100 µm thick. Hymenial surface tuberculate, white to pale gray when fresh, pale gray to cream on drying, with cracking. Margin sterile, narrow, and gray.

Hyphal system—Monomitic, generative hyphae with clamp connections, colorless, thin-walled, frequently branched, interwoven, 2.5–4.5 µm in diameter; IKI-, CB-; tissues unchanged in KOH.

Hymenium—Cystidia moniliform, thin-walled, 28–60 µm × 6.5–10.5 µm; basidia clavate to subcylindrical, slightly constricted in the middle to somewhat sinuous, with 4 sterigmata and a basal clamp connection, 21.5–31 µm × 5–7.5 µm.

Spores—Basidiospores ellipsoid to cylindrical, colorless, thin-walled, smooth, with irregular vacuole inside, IKI-, CB-, (10.5–)11–13.5(–14) µm × 4.5–5.5(–6) µm, L = 12.52 µm, W = 5.18 µm, Q = 2.42 (*n* = 60/2).

Additional specimens examined—China, Yunnan Province, Puer, Zhenyuan County, Heping Town, Liangzizhai, E 101°25′, N 23°56′, 2246 m asl., on fallen angiosperm branch, leg. C.L. Zhao, 15 Jan 2018, C.L. Zhao 5844 (SWFC).

Hyphoderma microporoides C.L. Zhao and Q.X. Guan sp. nov. Figures 6 and 7.

Figure 6. *Hyphoderma microporoides* (holotype) (**A**): basidiomata on the substrate (**B**) and scattered pinholes. Bars: **A** = 2 cm, **B** = 1 mm.

MycoBank no.: MB 839277.

Holotype—China, Yunnan Province, Chuxiong, Zixishan Forestry Park, E 101°24′, N 25°01′, 2313 m asl., on fallen angiosperm trunk, leg. C.L. Zhao, 30 June 2018, C.L. Zhao 6857 (SWFC).

Etymology—*microporoides* (Lat.): referring to the scattered pinholes on the hymenophore that are visible under hand lens.

Fruiting body—Basidiomata annual, resupinate, adnate, without odor and taste when fresh, cottony when fresh, fragile upon drying, and up to 22 cm long, 2.5 cm wide, and 50–100 μm thick. Hymenial surface smooth with scattered pinholes visible under hand lens, cream to pale buff when fresh, and slightly buff upon drying. Margin sterile, indistinct, and white to cream.

Hyphal system—Monomitic, generative hyphae with clamp connections, colorless, thin-walled, frequently branched, interwoven, 3–5 μm in diameter, IKI-, CB-; tissues unchanged in KOH.

Hymenium—Halocystidia capitate, thin-walled, smooth, 18–51 μm × 4.5–7 μm; basidia clavate, constricted, somewhat sinuous, with 4 sterigmata and a basal clamp connection, 18.5–29.5 μm × 5–7 μm.

Spores—Basidiospores cylindrical to allantoid, colorless, thin-walled, smooth, with oil drops inside, IKI-, CB-, 8.5–10(–10.5) µm × 2.5–3.5(–4) µm, L = 9.29 µm, W = 3.24 µm, Q = 2.87 (*n* = 30/1).

Additional specimens examined—China, Yunnan Province, Puer, Jingdong County, Taizhong Town, Ailaoshan Ecological Station, E 100°56′, N 24°29′, 1938 m asl., on fallen angiosperm branch, leg. C.L. Zhao, 25 August 2018, C.L. Zhao 8695 (SWFC).

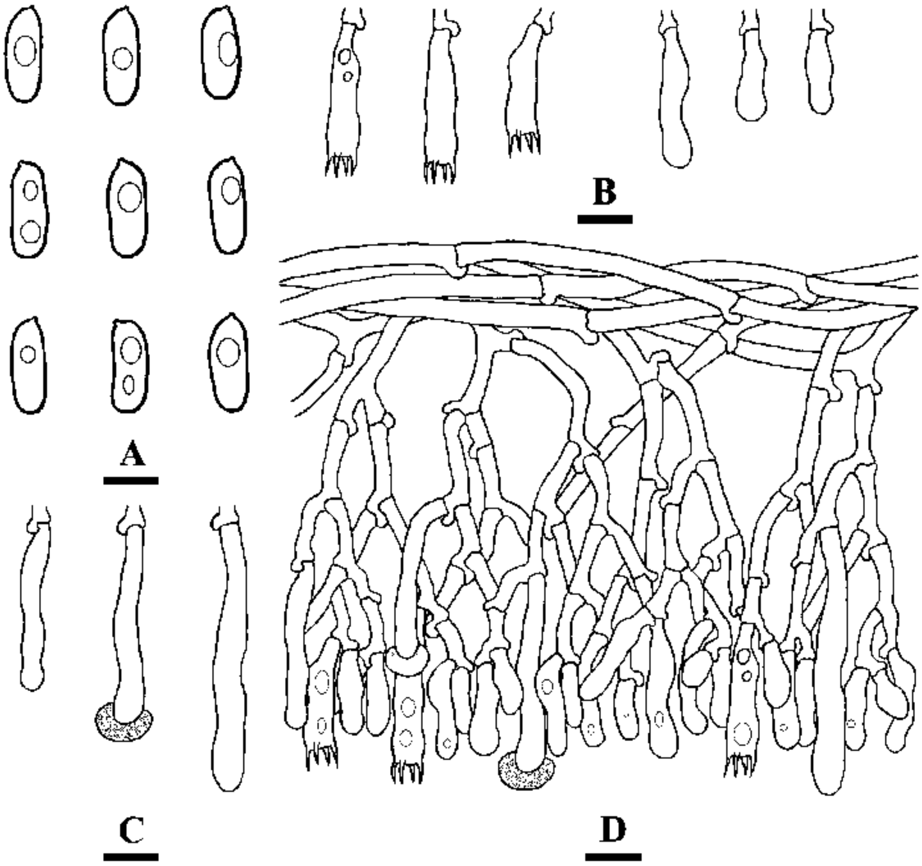

Figure 7. Microscopic structures of *Hyphoderma microporoides* (holotype) (**A**): basidiospores (**B**), basidia and basidioles (**C**), and cystidia (**D**). A section of hymenium. Bars: **A** = 5 µm, **B**–**D** = 10 µm.

4. Discussion

In the present study, three new species, *Hyphoderma crystallinum*, *H. membranaceum*, and *H. microporoides* are described based on phylogenetic analyses and morphological characteristics.

Phylogenetically, the family-level classification of the Polyporales (Basidiomycota) amplified nLSU, nITS, and rpb1 genes across the Polyporales, was employed, in which four species *Hyphoderma macaronesicum*, *H. medioburiense* (Burt) Donk, *H. mutatum* (Peck) Donk, and *H. setigerum*, nested into family Hyphodermataceae within the residual polyporoid clade [19]. In the present study, three new taxa clustered into *Hyphoderma*, in which *Hyphoderma crystallinum* was sister to *H. variolosum*, *H. microporoides* grouped closely with *H. nemorale,* and *H. membranaceum* grouped with *H. sinense* and *H. transiens* (Bres.) Parmasto (Figure 1). However, morphologically, *H. variolosum* differs from *H. crystallinum* by its narrower tubular cystidia (40–50 µm × 4–6 µm) [38]; *H. nemorale* is separated from *H. microporoides* by having the colliculose hymenial surface, wider moniliform cystidia (35–70 µm × 7–8 µm) and basidiospores (9.5–14 µm × 4–5 µm) [27]; *H. sinense* differs from *H. membranaceum* by having the encrusted cystidia and smaller basidiospores (8–11.5 µm × 3–5 µm) [25], and another species *H. transiens* differs in its odontioid hymenial surface and narrower basidiospores (9–13 µm × 3–4.5 µm) [39].

Morphologically, *Hyphoderma ayresii* (Berk. ex Cooke) Boidin and Gilles, *H. cremeum* Sheng H. Wu and *H. rimulosum* Sheng H. Wu are similar to *H. crystallinum* by having encrusted cystidia. However, *H. ayresii* differs in its larger encrusted cystidia (70–130 µm × 13–20 µm) and wider basidiospores (9.5–12.5 µm × 6–8 µm) [38]; *H. cremeum* differs from *H. crystallinum* by having both larger encrusted cystidia (40–90 µm × 10–15 µm) and basidia (35–50 µm × 6.5–8 µm) [40]; *H. rimulosum* is separated from *H. crystallinum* by smaller basidiospores (6–7 µm × 3.9–4.1 µm) [41]. *Hyphoderma incrustatum* K.H. Larss., *H. medioburiense*, *H. multicystidium* (Hjortstam and Ryvarden) Hjortstam and Tellería and *H. roseocremeum* (Bres.) Donk are similar to *H. crystallinum* by having tubular cystidia. However, *H. incrustatum* differs from *H. crystallinum* by the porulose hymenial surface and the larger tubular cystidia (50–80 µm × 6–10 µm) [42]; *H. medioburiense* is separated from *H. crystallinum* by the porulose hymenial surface and the larger tubular cystidia (60–100 µm × 7–10 µm) [8]; *H. multicystidium* differs in its larger tubular cystidia (60–80 µm × 5–7 µm), larger basidia (35–50 µm × 5–7 µm) and smaller basidiospores (8–10 µm × 4.5–5 µm) [43]; *H. roseocremeum* differs from *H. crystallinum* by having larger tubular cystidia (80–100 × 6–9 µm) and smaller basidiospores (8–12 µm × 3–4 µm) [8].

Hyphoderma litschaueri, *H. moniliforme* (P.H.B. Talbot) Manjón, G. Moreno and Hjortstam, *H. paramacaronesicum* Tellería et al., *H. prosopidis* (Burds.) Tellería et al. and *H. sinense* are similar to *H. membranaceum* by having moniliform or apically moniliform cystidia. However, *H. litschaueri* differs from *H. membranaceum* by having larger moniliform cystidia (60–100 µm × 6–8 µm) and narrower basidiospores (9–12 µm × 3–4 µm) [44]; *H. moniliforme* differs from *H. membranaceum* by having smaller basidiospores (8–9 µm × 3.5–4 µm) [27]; *H. paramacaronesicum* differs in its having both larger moniliform cystidia (70–124 µm × 8–13 µm) and basidia (40−48 µm × 6−9 µm), and wider basidiospores (12–15 µm × 5.5–7 µm) [14]; *H. prosopidis* differs from *H. membranaceum* by the arachnoid to farinaceous hymenial surface and larger basidia (40−45 µm × 8−11 µm) [17]; and *H. sinense* differs in its having encrusted cystidia (18.5–38 µm × 6–11 µm) and smaller basidiospores (8–11.5 µm × 3–5 µm) [25].

Hyphoderma clavatum Sheng H. Wu, *H. etruriae* Bernicchia, *H. incrustatum*, *H. orphanellum* (Bourdot & Galzin) Donk, and *H. subclavatum* Sheng H. Wu are similar to *H. microporoides* by having capitate cystidia. However, *H. clavatum* differs from *H. microporoides* by the tuberculate hymenial surface and larger basidiospores (10–13 µm × 4.2–5.2 µm) [41]; *H. etruriae* differs from *H. microporoides* by the grandinioid hymenial surface and wider basidiospores (9–11 µm × 5.5–6.5 µm) [45]; *H. incrustatum* differs in having larger basidiospores (11–14 µm × 4–5 µm) [42]; *H. orphanellum* differs from *H. microporoides* by having larger capitate cystidia (50–80 µm × 8–10 µm) and wider basidiospores (8–10 µm × 5–6 µm) [8]; *H. subclavatum* is separated from *H. microporoides* by having both larger basidia (40–55 µm × 7–8 µm) and basidiospores (10–12 µm × 4.2–5.3 µm) [41].

Hyphoderma species are an extensively studied group [10,46], mainly distributed in Europe (e.g., Austria, Russia, France, Germany, Poland, UK, The Netherlands, Portugal, Sweden, Italy, Denmark, Norway, Finland, Spain) (Figure 8) and mainly found on hardwood, although a few species grow on coniferous wood. Many species of *Hyphoderma* were found in Europe, but most of them have not been reported in northern China (Figure 8), in which we presumed that *Hyphoderma* are undersampled by mycologists. Several studies on new wood-decaying fungi of *Hyphoderma* from China have been reported [15,40,41,46], in which 26 *Hyphoderma* species were reported, *H. acystidiatum* Sheng H. Wu, *H. clavatum*, *H. cremeoalbum* (Höhn. and Litsch.) Jülich, *H. cremeum*, *H. definitum* (H.S. Jacks.) Donk, *H. densum* Sheng H. Wu, *H. fissuratum*, *H. floccosum* C.L. Zhao and Q.X. Guan, *H. litschaueri*, *H. crystallinum*, *H. medioburiense*, *H. microcystidium* Sheng H. Wu, *H. microporoides*, *H. moniliforme*, *H. mopanshanense*, *H. nemorale*, *H. obtusiforme* J. Erikss. and Å. Strid, *H. pinicola*, *H. rimulosum*, *H. setigerum*, *H. sibiricum* (Parmasto) J. Erikss. and Å. Strid, *H. sinense*, *H. subclavatum*, *H. subsetigerum* Sheng H. Wu, *H. transiens,* and *H. membranaceum* [8,18,25,27,29,40,41,46]. Further studies should focus on the relationships between the host and *Hyphoderma* species, as well as trying to better understand the evolutionary directions between plant and *Hyphoderma* species. The researches on the phylogeny of *Hyphoderma*, as well as many fungal studies on the molecular systematics [47–49], will be useful to push the further research on fundamental research and applied research of fungi. More species of *Hyphoderma* should be found in subtropical and tropical Asia as it was shown that wood-inhabiting fungi are rich in tropical China [50,51].

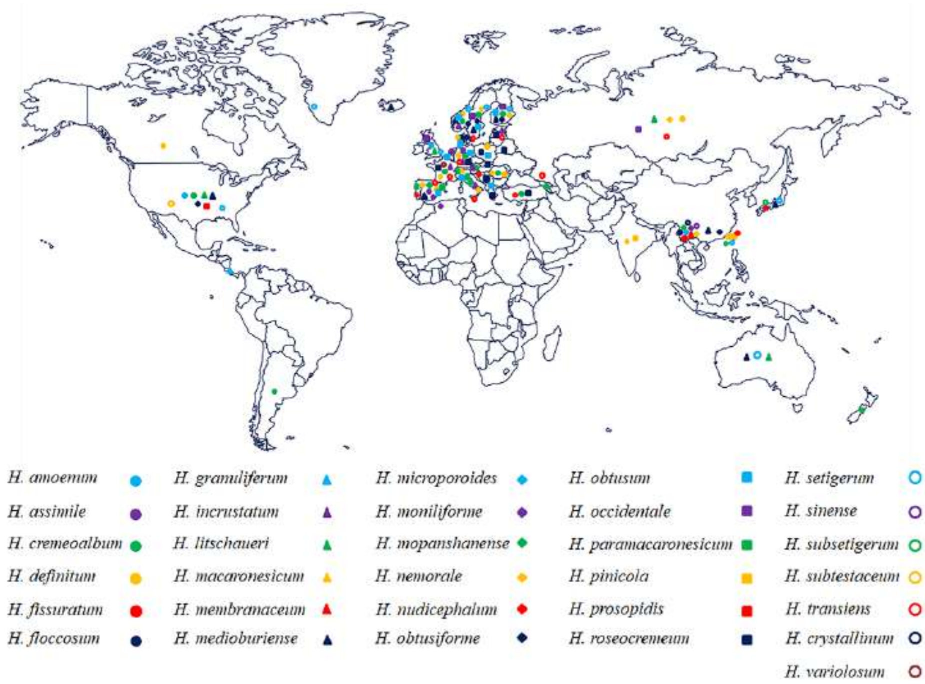

Figure 8. Geographic distribution of *Hyphoderma* species treated in the phylogenetic tree.

Key to 26 accepted species of *Hyphoderma* in China

1. Cystidia absent 2
2. Cystidia present 5
3. Hymenial surface grandinioid *H. acystidiatum*
4. Hymenial surface smooth 3
5. Basidiospores > 10.5 µm in length *H. densum*
6. Basidiospores < 10.5 µm in length 4
7. Hymenophore cracked; basidiospores > 8.5 µm in length *H. fissuratum*
8. Hymenophore uncracked; basidiospores < 8.5 µm in length *H. sibiricum*
9. Hymenophore smooth 6
10. Hymenophore tuberculate, porulose, grandinioid, or odontoid 14
11. Two types of cystidia present 7
12. One type of cystidia present 8
13. Moniliform cystidia absent *H. microcystidium*
14. Moniliform cystidia present *H. sinense*
15. Hymenophore uncracked 9
16. Hymenophore cracked 10
17. Basidiospores > 11 µm in length *H. definitum*
18. Basidiospores < 11 µm in length *H. microporoides*
19. Cystidia moniliform 11
20. Cystidia cylindrical 12
21. Basidiospores > 9 µm in length *H. litschaueri*
22. Basidiospores < 9 µm in length *H. moniliforme*
23. Basidiospores ellipsoid < 10 µm in length *H. rimulosum*
24. Basidiospores cylindrical > 10 µm in length 13
25. Basidiospores > 12 µm in length *H. cremeum*

26. Basidiospores < 12 μm in length *H. subclavatum*
27. Hymenophore odontoid or grandinioid 15
28. Hymenophore tuberculate, porulose 16
29. Hymenophore odontoid, basidiospores > 9 μm in length *H. transiens*
30. Hymenophore grandinioid, basidiospores < 9 μm in length *H. subsetigerum*
31. Cystidia of two types 17
32. Cystidia of one type 19
33. Septate cystidia absent *H. crystallinum*
34. Septate cystidia present 18
35. Basidia 2-sterigmata, basidiospores > 13 μm in length *H. pinicola*
36. Basidia 4-sterigmata, basidiospores < 13 μm in length *H. floccosum*
37. Septate cystidia present 20
38. Septate cystidia absent 21
39. Hymenophore porulose to pilose, basidia < 5 μm in width *H. mopanshanense*
40. Hymenophore tuberculate, basidia > 5 μm in width *H. setigerum*
41. Hymenophore porulose *H. obtusiforme*
42. Hymenophore tuberculate, colliculose 22
43. Cystidia > 30 μm in length 23
44. Cystidia < 30 μm in length *H. cremeoalbum*
45. Basidia > 30 μm in length 24
46. Basidia < 30 μm in length 25
47. Hymenophore cracking, cystidia < 10 μm in width *H. medioburiense*
48. Hymenophore not cracking, cystidia > 10 μm in width *H. clavatum*
49. Hymenophore colliculose *H. nemorale*
50. Hymenophore tuberculate *H. membranaceum*

Author Contributions: Conceptualization, C.-L.Z.; methodology, C.-L.Z. and Q.-X.G.; software, C.-L.Z. and Q.-X.G.; validation, C.-L.Z. and Q.-X.G.; formal analysis, C.-L.Z. and Q.-X.G.; investigation, C.-L.Z. and Q.-X.G.; resources, C.-L.Z.; writing—original draft preparation, C.-L.Z. and Q.-X.G.; writing—review and editing, C.-L.Z. and Q.-X.G.; visualization, C.-L.Z. and Q.-X.G.; supervision, C.-L.Z.; project administration, C.-L.Z.; funding acquisition, C.-L.Z. All authors have read and agreed to the published version of the manuscript.

Funding: This research was funded by the Yunnan Fundamental Research Project, grant number 202001AS070043.

Institutional Review Board Statement: Not applicable for studies involving humans or animals.

Informed Consent Statement: Not applicable for studies involving humans.

Data Availability Statement: Publicly available datasets were analyzed in this study. This data can be found here: [https://www.ncbi.nlm.nih.gov/; https://www.mycobank.org/page/Simple%20names%20search; http://purl.org/phylo/treebase, submission ID 27983; accessed on 16 April 2021].

Conflicts of Interest: The authors declare no conflict of interest.

References

1. James, T.Y.; Stajich, J.E.; Hittinger, C.T.; Rokas, A. Toward a fully resolved fungal tree of life. *Annu. Rev. Microbiol.* **2020**, *74*, 1–23. [CrossRef]
2. Lutzoni, F.; Nowak, M.D.; Alfaro, M.E.; Reeb, V.; Miadlikowska, J.; Krug, M.; Arnold, A.E.; Lewis, L.A.; Swofford, D.L.; Hibbett, D.; et al. Contemporaneous radiations of fungi and plants linked to symbiosis. *Nat. Commun.* **2018**, *9*, 5451. [CrossRef]
3. Rokas, A.; Wisecaver, J.H.; Lind, A.L. The birth, evolution and death of metabolic gene clusters in fungi. *Nat. Rev. Microbiol.* **2018**, *16*, 731–744. [CrossRef]
4. Hibbett, D.S. The invisible dimension of fungal diversity. *Science* **2016**, *351*, 1150–1151. [CrossRef] [PubMed]
5. Blackwell, M. The Fungi: 1, 2, 3... 5.1 million species? *Am. J. Bot.* **2011**, *98*, 426–438. [CrossRef]
6. Hawksworth, D.L.; Lücking, R. Fungal diversity revisited: 2.2 to 3.8 million species. *Microbiol. Spectr.* **2017**, *5*. [CrossRef]
7. Floudas, D.; Binder, M.; Riley, R.; Barry, K.; Blanchette, R.A.; Henrissat, B.; Martínez, A.T.; Otillar, R.; Spatafora, J.W.; Yadav, J.S.; et al. The Paleozoic origin of enzymatic lignin decomposition reconstructed from 31 fungal genomes. *Science* **2012**, *336*, 1715–1719. [CrossRef] [PubMed]

8. Donk, M.A. Notes on resupinate Hymenomycetes IV. *Fungus* **1957**, *27*, 1–29.
9. Wallroth, C.F.W. *Flora Cryptogamica Germaniae*; Nabu Press: Nürnberg, Germany, 1833; Volume 2, pp. 1–923.
10. Bernicchia, A.; Gorjón, S.P. *Fungi Europaei 12: Corticiaceae s.l.*; Edizioni Candusso: Alassio, Italy, 2010.
11. Nakasone, K.K. Type studies of corticioid Hymenomycetes described by Bresadola. *Cryptogam. Mycol.* **2008**, *29*, 231–257. [CrossRef]
12. Wu, S.H.; Nilsson, H.R.; Chen, C.T.; Yu, S.Y.; Hallenberg, N. The white-rotting genus *Phanerochaete* is polyphyletic and distributed throughout the phlebioid clade of the Polyporales (Basidiomycota). *Fungal Divers.* **2010**, *42*, 107–118. [CrossRef]
13. Baltazar, J.M.; Silveira, R.M.B.; Rajchenberg, M. Type studies of J. Rick's corticioid Homobasidiomycetes (Agaricomycetes, Basidiomycota) housed in the Herbarium Anchieta (PACA). *Phytotaxa* **2016**, *255*, 101–132. [CrossRef]
14. Martín, M.P.; Zhang, L.F.; Fernández-López, J.; Dueñas, M.; Rodríguez-Armas, J.L.; Beltrán-Tejera, E.; Telleria, M.T. *Hyphoderma paramacaronesicum* sp. nov. (Meruliaceae, Polyporales, Basidiomycota), a cryptic lineage to *H. macaronesicum*. *Fungal Syst. Evol.* **2018**, *2*, 57–68. [CrossRef] [PubMed]
15. Ma, X.; Huang, R.X.; Zhang, Y.; Zhao, C.L. *Hyphoderma fissuratum* and *H. mopanshanense* spp. nov. (Polyporales) from southern China. *Mycoscience* **2021**, *62*, 36–41. [CrossRef]
16. Larsson, K.H. Re-thinking the classification of corticioid fungi. *Mycol. Res.* **2007**, *111*, 1040–1063. [CrossRef] [PubMed]
17. Telleria, M.T.; Dueñas, M.; Beltrán-Tejera, E.; Rodríguez-Armas, J.L.; Martín, M.P. A new species of *Hyphoderma* (Meruliaceae, Polyporales) and its discrimination from closely related taxa. *Mycologia* **2012**, *104*, 1121–1132. [CrossRef]
18. Yurchenko, E.; Wu, S.H. *Hyphoderma formosanum* sp. nov. (Meruliaceae, Basidiomycota) from Taiwan. *Sydowia* **2014**, *66*, 19–23.
19. Justo, A.; Miettinen, O.; Floudas, D.; Ortiz-Santana, B.; Sjökvist, E.; Linder, D.; Nakasone, K.; Niemelä, T.; Larsson, K.; Ryvarden, L.; et al. A revised family-level classification of the Polyporales (Basidiomycota). *Fungal Biol.* **2017**, *121*, 798–824. [CrossRef] [PubMed]
20. Petersen, J.H. *Farvekort. The Danish Mycological Society's Colour-Chart*; Foreningen til Svampekundskabens Fremme: Greve, Denmark, 1996; pp. 1–6.
21. Dai, Y.C. Polypore diversity in China with an annotated checklist of Chinese polypores. *Mycoscience* **2012**, *53*, 49–80. [CrossRef]
22. Zhao, C.L.; Wu, Z.Q. *Ceriporiopsis kunmingensis* sp. nov. (Polyporales, Basidiomycota) evidenced by morphological characters and phylogenetic analysis. *Mycol. Prog.* **2017**, *16*, 93–100. [CrossRef]
23. White, T.J.; Bruns, T.; Lee, S.; Taylor, J. Amplification and direct sequencing of fungal ribosomal RNA genes for phylogenetics. *PCR Protoc. Guide Methods Appl.* **1990**, *18*, 315–322. [CrossRef]
24. Vu, D.; Groenewald, M.; Vries, M.; Gehrmann, T.; Stielow, B.; Eberhardt, U.; Al-Hatmi, A.; Groenewald, J.Z.; Cardinali, G.; Houbraken, J.; et al. Large-scale generation and analysis of filamentous fungal DNA barcodes boosts coverage for kingdom Fungi and reveals thresholds for fungal species and higher taxon delimitation. *Stud. Mycol.* **2019**, *92*, 135–154. [CrossRef] [PubMed]
25. Guan, Q.X.; Zhao, C.L. Two new corticioid species: *Hyphoderma sinense* and *H. floccosum* spp. nov. (Hyphodermataceae, Polyporales) from southern China. *Mycosystema* **2021**, in press. [CrossRef]
26. Floudas, D.; Hibbett, D.S. Revisiting the taxonomy of *Phanerochaete* (Polyporales, Basidiomycota) using a four gene dataset and extensive ITS sampling. *Fungal Biol.* **2015**, *119*, 679–719. [CrossRef] [PubMed]
27. Yurchenko, E.; Wu, S.H. *Hyphoderma moniliforme* and *H. nemorale* (Basidiomycota) newly recorded from China. *Mycosphere* **2015**, *6*, 113–121. [CrossRef]
28. Nilsson, R.H.; Hallenberg, N.; Nordén, B.; Maekawa, N.; Wu, S.H. Phylogeography of *Hyphoderma setigerum* (Basidiomycota) in the Northern Hemisphere. *Mycol. Res.* **2003**, *107*, 645–652. [CrossRef] [PubMed]
29. Yurchenko, E.; Wu, S.H. *Hyphoderma pinicola* sp. nov. of *H. setigerum* complex (Basidiomycota) from Yunnan, China. *Bot. Stud.* **2014**, *55*, 71–78. [CrossRef]
30. Telleria, M.T.; Duenas, M.; Melo, I.; Hallenberg, N.; Martin, M.P. A re-evaluation of *hypochnicium* (polyporales) based on morphological and molecular characters. *Mycologia* **2010**, *102*, 1426–1436. [CrossRef] [PubMed]
31. Wu, F.; Chen, J.J.; Ji, X.H.; Vlasák, J.; Dai, Y.C. Phylogeny and diversity of the morphologically similar polypore genera *Rigidoporus*, *Physisporinus*, *Oxyporus* and *Leucophellinus*. *Mycologia* **2017**, *109*, 749–765. [CrossRef]
32. Hall, T.A. BioEdit: A user-friendly biological sequence alignment editor and analysis program for Windows 95/98/NT. *Nucleic Acids Symp. Ser.* **1999**, *41*, 95–98. [CrossRef]
33. Swofford, D.L. *PAUP*: Phylogenetic Analysis Using Parsimony (*and Other Methods)*; Version 4.0b10; Sinauer Associates: Sunderland, MA, USA, 2002.
34. Felsenstein, J. Confidence intervals on phylogenetics: An approach using bootstrap. *Evolution* **1985**, *39*, 783–791. [CrossRef] [PubMed]
35. Miller, M.A.; Holder, M.T.; Vos, R.; Midford, P.E.; Liebowitz, T.; Chan, L.; Hoover, P.; Warnow, T. The CIPRES Portals. CIPRES. Available online: http://www.phylo.org/sub_sections/portal (accessed on 9 September 2020).
36. Nylander, J.A.A. *MrModeltest v2. Program Distributed by the Author*; Evolutionary Biology Centre, Uppsala University: Uppsala, Sweden, 2004.
37. Ronquist, F.; Huelsenbeck, J.P. MrBayes 3: Bayesian phylogenetic inference under mixed models. *Bioinformatics* **2003**, *19*, 1572–1574. [CrossRef] [PubMed]
38. Boidin, J.; Gilles, G. Basidiomycètes Aphyllophorales de l'Île de La Réunion. XVI. Les genres *Hyphoderma*, *Hyphodermopsis*, *Chrysoderma* nov. gen. et *Crustoderma*. *Cryptogam. Mycol.* **1991**, *12*, 97–132.

39. Parmasto, E. *Conspectus Systematis Corticiacearum*; Institutum Zoologicum et Botanicum Academiae Scientiarum RPSS Estonicae: Tartu, Estonia, 1968.
40. Wu, S.H. New species of *Hyphoderma* from Taiwan. *Mycologia* **1997**, *89*, 132–140. [CrossRef]
41. Wu, S.H. New species and new records of *Hyphoderma* (Basidiomycotina) from Taiwan. *Bot. Bull. Acad. Sin.* **1997**, *38*, 63–72.
42. Larsson, K.H. Two new species in *Hyphoderma*. *Nord. J. Bot.* **1998**, *18*, 121–127. [CrossRef]
43. Tellería, M.T. Annotated list of the Corticiaceae, sensu lato (Aphyllophorales, Basidiomycotina), for Peninsular Spain and Balearic Islands. *Bibl. Mycol.* **1990**, *135*, 1–152.
44. Eriksson, J.; Ryvarden, L. *The Corticiaceae of North Europe*; Fungiflora: Oslo, Norway, 1975; Volume 3, pp. 288–546.
45. Bernicchia, A. *Hyphoderma etruriae* sp. nov. (Corticiaceae, Basidiomycetes) from the natural reserve of Burano, Italy. *Mycotaxon* **1993**, *46*, 37–40.
46. Dai, Y.C. A revised checklist of corticioid and hydnoid fungi in China for 2010. *Mycoscience* **2011**, *52*, 69–79. [CrossRef]
47. Bhunjun, C.S.; Phukhamsakda, C.; Jeewon, R.; Promputtha, I.; Hyde, K.D. Integrating different lines of evidence to establish a novel Ascomycete genus and family (anastomitrabeculia, anastomitrabeculiaceae) in Pleosporales. *J. Fungi* **2021**, *7*, 94. [CrossRef]
48. Lambert, C.; Pourmoghaddam, M.J.; Cedeo-Sanchez, M.; Surup, F.; Stadler, M. Resolution of the *hypoxylon fuscum* complex (Hypoxylaceae, Xylariales) and discovery and biological characterization of two of its prominent secondary metabolites. *J. Fungi* **2021**, *7*, 131. [CrossRef]
49. Zhou, M.; Dai, Y.C.; Vlasák, J.; Yuan, Y. Molecular phylogeny and global diversity of the genus *Haploporus* (Polyporales, Basidiomycota). *J. Fungi* **2021**, *7*, 96. [CrossRef] [PubMed]
50. Cui, B.K.; Li, H.J.; Ji, X.; Zhou, J.L.; Song, J.; Si, J.; Yang, Z.L.; Dai, Y.C. Species diversity, taxonomy and phylogeny of Polyporaceae (Basidiomycota) in China. *Fungal Divers* **2019**, *97*, 137–392. [CrossRef]
51. Wu, F.; Yuan, H.S.; Zhou, L.W.; Yuan, Y.; Cui, B.K.; Dai, Y.C. Polypore diversity in South China. *Mycosystema* **2020**, *39*, 653–681. [CrossRef]